

Atmospheric Oxidation of PFAS by Hydroxyl Radical: A Density Functional Theory Study

Michael R. Dooley, Steven P. Nixon, Benjamin E. Payton,[‡] Mikayla A. Hudak,[‡] Fiona Odei, and Shubham Vyas*



Cite This: *ACS EST Air* 2024, 1, 1352–1361



Read Online

ACCESS |

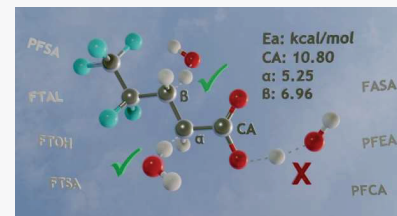
Metrics & More

Article Recommendations

Supporting Information

ABSTRACT: Per- and polyfluoroalkyl substances (PFAS) are persistent, widely spread, and harmful pollutants. They can travel through the air, be transformed by radicals, and deposit into water or onto surfaces. They enter the atmosphere via direct emission, degradation of precursors, or aerosol formation. A recent investigation found novel compounds in rainwater, meaning PFAS may undergo transformations in the atmosphere. These transformations might exhibit distinct behavior compared to more well-researched reactions, creating difficulties in the identification of any new compounds being produced. Using density functional theory (DFT), we simulated reactions of PFAS with a major atmospheric radical, the hydroxyl radical, revealing activation energies and other thermodynamic insights. The activation energies aid in predicting likely reactions and understanding speciation. Identifying new species can guide future analyses and remediation efforts. We focused on the nine most widely studied families of PFAS, finding that radical abstraction along the alkyl chain is favored over functional groups regardless of chain length. These results establish a new foundation for understanding PFAS transformations in the atmosphere, especially when decarboxylation is not followed.

KEYWORDS: *Per- and polyfluoroalkyl substances, PFAS, hydroxyl radical, atmospheric transformation, DFT*



INTRODUCTION

Per- and polyfluoroalkyl substances (PFAS) are persistent, ubiquitous, and harmful pollutants.¹ PFAS were initially developed for various commercial uses due to their hydrophobic, oleophobic, and surfactant properties. These substances are produced on a large scale for many different commercial applications due to their high thermal and chemical stability.² Unfortunately, this stability that made them so useful also makes them extremely recalcitrant environmental contaminants. These substances have perforated the environment and our bodies through multiple pathways.¹ PFAS cannot be easily broken down naturally or with existing wastewater treatment methods due to the strong carbon–fluorine bond.³ They tend to accumulate in organisms and have been detected in 98% of humans, raising concerns about their link to cancer and other environmental issues.⁴ They can reach the atmosphere through direct emission, aerosol formation, or by degradation of precursors.^{5–7} Atmospheric PFAS profiles show that some subclasses are likely to partition into the gas phase, depending on functional groups and the degree of fluorination.^{8,9} Once there, PFAS can undergo long-range transport in both gas and particulate phases, eventually brought back down by wet and dry deposition.¹⁰ The discovery of PFAS in distant, isolated areas like the Arctic and Antarctica are evidence of this long-range transport, as they are not produced naturally.^{11–14} Transport and deposition of PFAS raise concerns due to their adverse effects on ecosystems and human health.^{4,15–17}

The exact amount and variety of PFAS in the atmosphere remain uncertain. Previous studies have quantified a variety of PFAS in the atmosphere, but their analysis was limited to only searching for some of the most commonly produced PFAS.^{9,16,18} A recent investigation found novel compounds in rainwater, raising questions about potential chemical transformations in the atmosphere.¹⁹ In the same study, it was shown that these uncharacterized compounds may constitute the majority of PFAS in rainwater samples. Enhancing methods for identifying these compounds is gaining importance as these novel substances become more prevalent. The analytical challenges such as the lack of available PFAS standards hamper PFAS detection, quantification, and characterization in the environment. While improvements in analysis have been made, only a small portion of the total PFAS have been directly detected with targeted approaches.²⁰ Nontarget analysis shows promise, but researchers have varying confidence in the resulting identified structures, and the technique requires further development.¹⁹ To address these challenges and improve our understanding of the mechanisms involved, a computational approach examining

Received: March 26, 2024

Revised: September 26, 2024

Accepted: September 27, 2024

Published: October 10, 2024



interactions of PFAS with atmospheric radicals can help predict speciation and provide critical information to assist in future analysis.

This study examines the reaction between PFAS and the hydroxyl radical by employing density functional theory (DFT). Hydroxyl radicals were used because they are ubiquitous in the atmosphere and they play a role in environmental transformations of aqueous film forming foams (AFFF) which contain PFAS.^{13,14,21,22} While the direct oxidation of PFAS by hydroxyl radicals in the aqueous phase has been a subject of debate, these radicals are integral to the chemical transformation mechanisms of PFAS in diverse oxidative conditions.³ In this study, we explicitly study hydrogen atom abstraction by a hydroxyl radical in the context of PFAS. The abstraction generates a radical on PFAS, initiating its atmospheric chemical transformation. Understanding this radical initiation step is a key initial approach to comprehending the observed complex speciation in the atmosphere. The DFT computations can provide crucial parameters such as bond dissociation energies, reaction enthalpies, and associated activation energies.^{23–25} Comparing activation energies helps identify which reaction pathways are more probable and provides insight into speciation.

In this paper, we have performed hydroxyl radical remediated reaction with nine PFAS classes and subclasses, namely, perfluoroalkyl carboxylic acids (PFCA), perfluoroalkyl sulfonic acids (PFSA), fluorotelomer carboxylic acids (FTCA), fluorotelomer sulfonic acids (FTSA), fluorotelomer alcohols (FTOH), perfluoroalkyl sulfonamides (FASA), perfluoroalkyl ether acids (PFEA), perfluoroalkyl diether acids (Double-PFEA), and perfluoroalkyl aldehydes (PFAL). Fluoroalkyl chain length was varied to match the variety of different chain lengths found in the environmental samples such as rainwater.^{18,26} The role of α carbon substitution by trifluoromethyl groups was also investigated because PFAS replacement molecules such as the regulated hexafluoropropylene oxide dimer acid (HFPO-DA, trade name GenX) were produced with this substitution and they have also been found in rainwater.^{26,27} The results of this study show no noticeable chain length dependence for most families, and abstraction of a hydrogen atom through the alkylated chain is always preferred when compared to abstraction from the functional group. These results serve as the fundamental basis to develop new mechanisms for PFAS transformations in the atmosphere.

MATERIALS AND METHODS

DFT calculations were performed using Gaussian 16 software suite employing the M06-2X/6-311++G(2d,2p) level of theory.²⁸ The selection of M06-2X functional was based on its demonstrated accuracy for main-group thermochemistry and kinetics, particularly in the context of noncovalent interactions like hydrogen abstraction, rendering it a highly suitable functional for this study.²⁹ Alternative functional and basis set combinations were explored, but the M06-2X/6-311++G(2d,2p) setup proved to be the most efficient choice for both the PFAS and radical systems under examination (see Supporting Information for more information). We expect the electron density of a PFAS molecule in the atmosphere to be influenced by other coconstituents interacting with PFAS during hydroxyl radical reactions. Hence, the SMD implicit solvation model for water was employed to consider the microsolvation environment.³⁰ We validated this choice of implicit solvation for this experiment, the details of which can

be found in Figure S1 and the associated discussion. However, it has been shown that in the atmosphere hydroxyl can have sparse interactions with water,³¹ meaning the polar PFAS molecules only have sparse interactions as well, and that the SMD solvation model may not be the most accurate treatment for the conditions. While the SMD model was found to be acceptable for this investigation, the researchers recommend utilizing a few explicit water molecules instead of any implicit solvation in future studies.

All of the stationary points and transition states were characterized by obtaining second derivatives of energy analytically and identification of no or one imaginary vibrational mode, respectively. To characterize the nature of transition states, the intrinsic reaction coordinate (IRC) method was employed. Furthermore, using the imaginary vibrational modes, both reactant and product complexes were obtained that were subsequently used in the calculation of activation barriers.

To provide a complete analysis of this reaction, it was necessary to examine the effects of different conformations on the activation barriers. It has been demonstrated in literature that hydrogen abstraction reactions can be influenced strongly by different conformations.³² However, many PFAS studied here do not have the ability to freely rotate around as many carbon–carbon bonds as normal alkanes due to their rigid helical conformations, but it has been demonstrated they have some conformational variability for hydrogen abstraction.^{33–35} For certain PFAS species, conformations have been found with unique intramolecular interactions which substantially distort their structures, however when these molecules are coordinated to a hydroxyl radical in these transition states these electrostatically interacting conformers are not possible.^{36,37} Nevertheless, to evaluate the importance of conformation analysis for this study for this study, the constrained transition state randomization (CTSR) tool was employed to generate many different transition state conformations for a critical family (FTCA).³⁸ It was determined that the results presented herein are upheld without an in-depth conformational analysis due to overall small changes in geometry and energy (see Figure S3 and associated discussion for more details). While this initial conformational sampling is suitable for this investigation, future studies with a quantitative focus should include comprehensive conformational sampling.

RESULTS AND DISCUSSION

In this study, we investigate a range of PFAS subclasses, including completely fluorinated subclasses (PFCA, PFSA, and PFAL), fluorotelomer subclasses (FTCA, FTSA, and FTOH), subclasses with ether groups (PFEA, Double-PFEA), and sulfonamides (FASA). Figure 1 depicts the structural representations of each compound subclass, with “R” representing a fully fluorinated alkyl chain. Our investigation examined each H atom abstraction site on the molecule, which varied for each subclass. For example, 6:2 FTCA offers two potential hydrogen abstraction sites whereas in case of PFCA, only the carboxylic hydrogen can be abstracted. Additionally, for subclasses with a wide range of chain lengths present in rainwater, such as PFCA, we conducted simulations at multiple chain lengths to explore the potential impact of side chain. The length of the perfluoroalkyl chains can have an impact since perfluoroalkyl chains are helical in nature when compared to alkyl chains, and thus disturbing this helix with the creation of a radical will affect the energy of the system that would change

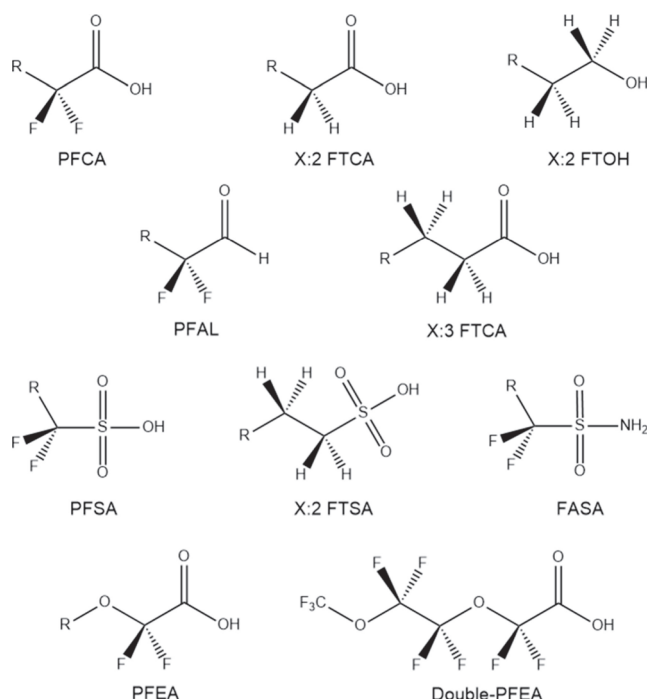


Figure 1. Different subclasses of PFAS investigated in this study. Note the R in structures denotes a completely fluorinated chain of varying length. The X in the fluorotelomers names denotes the number of carbons in the completely fluorinated alkyl chain.

depending on the amount of energy stored in the helical conformation.^{39,40} For most PFAS families, we also explored the substitution of fluorine with a trifluoromethyl group on the α carbon to assess its influence. In the case of FASA, we investigated the impact of substitution at the nitrogen center, as well.

Chain Length Dependence for PFCA. We began this work by evaluating the effect of fluorinated alkyl chain length on activation energy for the hydrogen abstraction in the case of PFCA. This narrow focus allows us to establish a baseline for comparison with other PFAS families. Figure 1 illustrates that PFCA offers only one potential site for hydrogen abstraction,

which resides within the carboxylic acid headgroup. These molecules are prevalent in the gas phase and are characterized by a diverse range of alkyl chain lengths, both in the gas phase and in rainwater.^{8,18,19}

As depicted in Figure 2, the activation barrier energy revealed no discernible correlation with the length of the alkyl chain. It is crucial to emphasize that any slight trend observed can be attributed to the margin of error associated with thermal corrections in quantum chemical computations. This error is a systematic error resulting from how quantum computations incorporate rotational degrees of freedom, and is relevant for all molecules in this study.⁴¹ More information about this systematic error can be found in the Supporting Information. Based on the deviation of the data points from the average, a gratuitous estimate of this error could be around 1.5 kcal/mol. This is evident when examining a plot of the bottom-of-the-well energies, which do not consider thermal corrections, against chain lengths, where no discernible trend emerges in Figure S2. These results align well with the prior literature, which also found no chain length dependence for electron addition at any position along the chain and reported that vertical attachment energy remained consistent regardless of chain length for PFCA.²⁴

Chain Length Dependence for FTCA. As shown in Figure 1, FTCA molecules offer two potential sites for hydrogen abstraction: one from the carboxylic acid headgroup and another from the α carbon, which features two hydrogen atoms in contrast to the fluorine atoms present in PFCA. The chain length dependence of abstraction from both the headgroup and alpha site were tested. As illustrated in Figure 2, the activation energy graphs for each site suggest a slight chain length dependence for FTCA. However, looking at a plot of the bottom-of-the-well energies shows no apparent chain length dependence, although there is a single outlier present (Figure S2 in Supporting Information). Therefore, we believe any apparent trends are introduced by the thermal correction errors, and we can confidently assert the absence of significant chain length dependence for FTCA.

Chain Length Dependence for PFEA. PFEA compounds are characterized by a limited range of chain lengths, primarily manifesting as a single variant known as HFPO-DA (trade

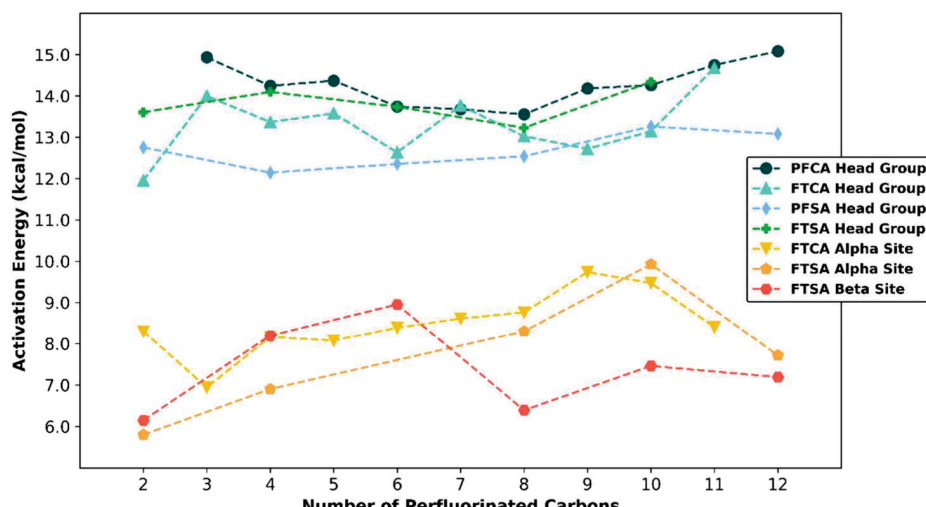


Figure 2. Calculated activation energies using Gibbs free energy as a function of the number of perfluorinated carbons in the chain for H atom abstraction by a hydroxyl radical. All energies calculated using the M06-2X/6-311++G(2d,2p) level of theory with the implicit solvation of water.

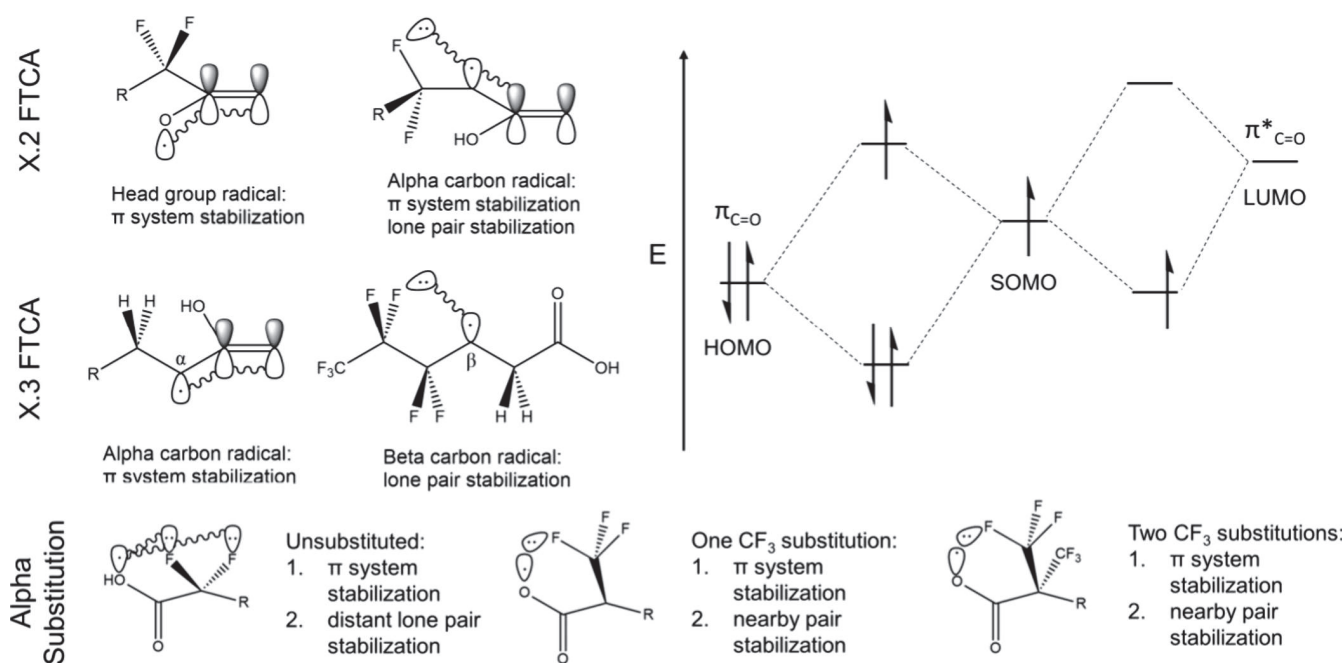


Figure 3. Illustration of possible interactions between the singly occupied molecular orbital of the radical center and other nearby orbitals in FTCA molecules. The top left depicts stabilizing interactions available to the molecule after abstraction has occurred from the headgroup, and the illustration on its right shows the interactions available to the molecule after the abstraction from the α carbon site. Similar interactions are shown for X.3 FTCA and PFCA with trifluoromethyl substitutions. The molecular orbital diagram illustrates that the radical can be stabilized by interacting with both filled and unfilled orbitals.

name GenX). Notably, the presence of ether linkages means that any abstraction or radical formation at the headgroup occurs farther from the extended hydrophobic tail, resulting in a reduced impact compared to PFCA counterparts. As a result, experimental investigations of these compounds focused on only a few select chain lengths. The data, presented in Table S1, agrees with this reasoning, showing only a 0.2 kcal/mol difference in PFEA molecules with two ethers (Double-PFEA). It is possible that changes in the length of the inner chain could have an effect but that was not included in this investigation.

Based on the results discussed above for PFCA, FTCA and PFEA, we conclude that hydrogen abstraction by a hydroxyl radical does not have a dependence on the length of the perfluoroalkyl chain in the gas phase. This conclusion holds significant importance, particularly in light of evidence suggesting that shorter chain PFCAAs are more resistant to degradation through many methods.⁴² In processes where surfaces play a pivotal role in PFCA degradation, hydrophobic and dispersive interactions exert a substantial influence on the chemical degradation of PFAS by interfering with the ability for the molecule to adsorb on the surface.⁴³ This is demonstrated by a decrease in effectiveness for a variety of degradation techniques as the chains get shorter.^{3,44} Yet, in the gas phase, surface coordination is unnecessary for the initiation step of hydrogen abstraction. As a result, the observed relationship between degradation effectiveness and chain length does not apply in this context.

Furthermore, the implication of these findings extends to the composition of atmospheric profiles of PFAS. The data shows that PFAS could be degraded at the same rate regardless of length, unlike what is observed in the aqueous phase.⁴⁴ This implies that it would be quicker to produce short and ultrashort chain PFCA compounds in the atmosphere than solution. As a result, the presence of short and ultrashort PFCA

may surpass what would be anticipated if one were to apply aqueous radical degradation rate constants to estimate airborne PFCA concentrations. Recent observations indicating the predominant presence of the shortest PFCA, trifluoroacetic acid, in the atmosphere and ice cores could be explained by this phenomenon.^{45,46}

Another noteworthy observation pertains to the activation energies involved in the process. Specifically, the Gibbs average activation energy for hydrogen abstraction from PFCA stands at approximately 14.3 kcal/mol. It is worth noting the proximity of this value to those reported in the literature for the activation energies associated with the radical oxidation of PFCA in solution, utilizing sulfate radical as the oxidant, where values range between 13.4 and 25.6 kcal/mol.^{47–51} This similarity suggests that the activation barrier for hydrogen atom abstraction from the carboxylic group in the gas phase is consistent with that encountered in the aqueous phase when PFCA undergoes one-electron transfer from the carboxylate group, mediated by the sulfate radical.

It is important to highlight the key distinction between these two scenarios. In the aqueous phase, the oxidation of PFCA is facilitated by the sulfate radical anion, whereas hydroxyl radical has been reported to be an inefficient agent for PFCA oxidation in the aqueous medium by itself.⁵² Conversely, our results show that in the gas phase the oxidation of PFCA via hydrogen atom abstraction by hydroxyl radical is a viable process. This divergence in oxidation pathways underscores the significance of the chemical environment in dictating the feasibility and mechanism of PFCA oxidative degradation.

Site Selectivity for H-Abstraction Reaction. In addition to the chain length dependence, we compared the activation energies of different abstraction sites on the same molecules. Many PFAS in the atmosphere are not completely fluorinated and therefore have additional hydrogens along the alkyl chain

that can be abstracted, such as the fluorotelomers. To get a complete picture of oxidation processes, it is important to evaluate the abstraction of these side chain hydrogens when present. First, FTCA was tested, as it has two abstraction sites as mentioned in the earlier section, the hydrogens on the α carbon and the hydrogen on the carboxylic acid headgroup. The data in **Figure 2** highlights a prominent energy preference for abstraction at the α carbon, along the alkyl chains, for FTCA.

The disparity between the average activation energy for carboxylic acid abstraction (13.3 kcal/mol) and alpha chain abstraction (8.5 kcal/mol) is substantial, amounting to a difference of 4.8 kcal/mol. This difference surpasses the expected error stemming from thermal corrections, which is estimated to be about 1.5 kcal/mol. Consequently, we can assert with confidence that the preference for side chain abstraction over H atom abstraction from the headgroup is well-founded. These findings are in excellent agreement with experimental results that found hydroxyl radical had a 100% yield when reacting with the α carbon of fluorotelomer alcohols.⁵³ This phenomenon markedly contrasts with what is typically observed in the surface dependent degradation, where the radical is preferentially formed at the headgroup.³ Furthermore, it can be clearly seen in **Figure 2** that across multiple families, the side chain abstraction is lower in activation energy than the carboxylic acid head groups.

A stereoelectronic explanation can be provided for the disparity in activation energies of H atom abstraction from the carboxylic acid and α carbon sites. Any filled or unfilled orbitals of similar energy that can physically align near the singly occupied radical orbital provide a stabilization by lowering the overall energy of the system, so the system with more of these interactions is lower in energy.⁵⁴ If the hydrogen is abstracted from the carboxylic acid, the resulting radical can be stabilized by interactions with the adjacent carbon–oxygen double bond π system, as depicted in **Figure 3**. However, if the radical is instead on the α carbon, it can have the same interaction with the π -system, but this position enables an additional stabilization effect through interaction with the lone pairs of the fluorine atoms on the beta carbon.

Subsequently, our investigation was extended to two X:3 FTCA molecules, which introduce a third potential abstraction site, the beta carbon. Our findings indicate that H-abstraction from the beta site requires lower energy compared to the carboxylic acid site. (**Table S2**) However, it is important to note that H-abstraction from the alpha site remains the preferred option over the beta site. This preference is attributed to the ability of a radical located on the α position to engage in electron donation into the π -system of the carbon–oxygen double bond, as visually depicted in **Figure 3**. Nevertheless, H-abstraction is preferred from the side chain.

This conclusion of side chain abstraction being preferential holds significant implications for the atmospheric fate of FTCA. Existing degradation pathways where oxidation takes place at the headgroup followed by Kolbe decarboxylation, ultimately leads to the regeneration of a carboxylic headgroup with shorter alkyl chain.³ However, initiation on the side chain would likely result in a different resulting reaction pathway, but this requires more research as it has only been observed for FTOH. This implies that in the atmospheric context, side chain abstraction may contribute, at least in part, to the formation of new substances. We hypothesize that detailed understanding of downstream products formed from H-

abstraction at the side chain in the atmosphere will lead to a better understanding of observed novel PFAS in the atmosphere, for which further research is warranted.

Our subsequent investigation focused on the FTSA compounds, which feature two hydrogenated carbons available for abstraction. We faced challenges in simulating hydrogen abstraction from the sulfonic acid headgroup, discussed below. However, we successfully conducted simulations for hydrogen abstraction from the headgroup, alpha, and beta carbon positions. When comparing the abstraction energies in **Figure 2**, the energy required for side-chain abstraction is significantly lower than that for the sulfonic acid headgroup. In alignment with FTCA, these results are in excellent agreement with literature and suggest side chain abstraction will be the predominant radical initiation step in the atmosphere.⁵³ Consequently, the occurrence of side chain abstractions in these previously unstudied reactions could be one route to the newly observed products and may challenge existing degradation pathways by introducing alternative reaction routes, but this requires further research.

Additionally, as illustrated in **Figure 2**, the activation energies for H atom abstractions from both alpha and beta carbons are about the same in contrast to what was observed for FTCA. This is likely due to the inability of the sulfonic headgroup to provide resonance stabilization to the carbon centered radical at the α carbon due to the geometric restraints in FTSA which were not present in FTCA. Perhaps this is important in the mechanisms forming the new PFAS found in rainwater, but it is unclear at this time.

Impact of Branching at the α Carbon. The third variable tested in this study is the impact of branching on the H atom abstraction reaction; in particular, substitution of trifluoromethyl groups onto the alpha carbons of the perfluoroalkyl chains. The introduction of an α carbon substitution noticeably influences the activation energy required for H-abstraction from the functional group. To elucidate this effect, we conducted simulations in which a trifluoromethyl group replaced a fluorine atom at the α carbon position. This was done for the PFCA and PFEA families, because these trifluoromethyl substitutions have been made on these subclasses historically to produce replacements that are supposedly easier to degrade (e.g., GenX). The results of these simulations are presented in **Figure S4**, revealing a discernible downward trend, showing that activation energy does decrease as trifluoromethyl groups are added onto the α carbon, albeit with relatively small differences in activation energies.

This observed trend can be rationalized from a stereoelectronic perspective. As stated above, nearby orbitals of similar energy provide a stabilization of the radical.⁵⁴ It is evident that the lone pairs associated with the fluorine atom could align with the orbital occupied by the radical, as illustrated in **Figure 3**. In the unaltered primary structure, there exists the possibility of some overlap between the singly occupied radical orbital and the lone pairs on the fluorine attached to the α carbon. However, these orbitals are somewhat distant in spatial proximity. When a trifluoromethyl group is introduced as a substitution at the α carbon position, a closer interaction emerges between the oxygen radical orbital and a nearby fluorine lone pair, resulting in a stronger interaction due to the reduced spatial separation of the orbitals.

In the case of the tertiary substituted compound, there are two opportunities for this enhanced interaction or the possibility of lone pairs of both trifluoromethyl groups

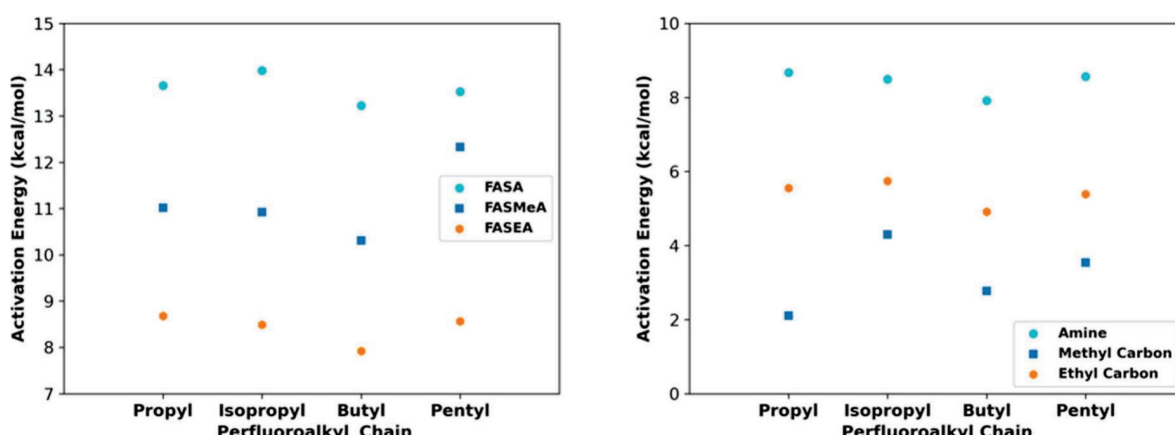


Figure 4. Amine site Gibbs activation energies with different perfluoroalkyl chains and head groups. The left graph shows activation energies for the amine site for three different FASA as a function of the perfluoroalkyl chain. The right graph shows activation energies for each abstraction site on the N-ethylsulfonamide as a function of the perfluoroalkyl chain. Energies were calculated using the M06-2X/6-311++G(2d,2p) level of theory with the implicit solvation of water.

interacting with the singly occupied molecular orbital of the oxygen atom, which imparts a slightly greater degree of stability compared to the secondary substitution. This hierarchy of stabilizing interactions is reflected in the activation energies of these substituted systems, with the primary structure exhibiting the highest activation energy, followed by secondary and tertiary substitutions in accordance with the strength of these interactions.

It is important to note that, in all of these molecules, the singly occupied molecular orbital resides in relatively closer proximity to the π and π^* orbitals associated with the carbon–oxygen double bond. This spatial proximity suggests the likelihood of a more robust interaction with these π orbitals. Consequently, the impact of the α carbon substitution appears relatively modest, as a stronger interaction is inherently present in all systems due to the proximity of the radical orbital to the relevant π orbitals.

The previously estimated 1.5 kcal/mol error in calculations, however, suggests that the observed trend within approximately 1.0 kcal/mol is likely not significant. The secondary substituted compound even has an increased activation energy for the PFEA data. We are therefore unable to make a concrete conclusion; therefore, alpha substitution likely does not have a large effect on the activation energies for hydrogen abstraction. The environmental implication of this is that this substitution, made in replacements like the GenX molecule to make it less recalcitrant, does not have an advantage in this degradation initiation reaction compared to similar molecules. Nevertheless, one can argue that a larger perfluoroalkyl side chain in place of a trifluoromethyl group can affect the energetics of the H atom abstraction reaction due to steric hindrance. However, this would not greatly alter the stereochemical argument presented here, and we did not explore this possibility in this study.

H Atom Abstraction from Sulfonic Acid Headgroup.

Hydrogen abstraction from PFSA compounds was also simulated, providing insights into chain length dependence and allowing for a comparison with PFCA abstraction. However, some challenges arose during the study of this family. In the existing literature, four transition states have been reported for hydrogen abstraction from sulfonic acids in the gas phase.⁵⁵ Initially, we tried to base our transition states on previously reported transition states but encountered two

problems. First, when we attempted to recreate these transition states the IRC analysis failed to provide the correct reactant complexes, raising concerns about the validity of these literature-reported states.⁵⁵ Second, a closer examination of the imaginary frequency in these transition states showed oscillations of the H atom between the sulfonic acid and the hydroxyl radical, as expected. However, these oscillations were coupled with the movement of the hydrogen of the hydroxyl group and the oxygen atom of the sulfonic acid, resulting in what appeared to be a rotational frequency or a strong rotation of the sulfur atom. It is also pertinent to note that experimental studies have indicated that radicals are unable to abstract a hydrogen from sulfonic acid in solution, further aligning with the difficulties we encountered in simulating these transition states.⁵⁶

We eventually succeeded in generating transition states for sulfonic acid headgroup hydrogen abstraction by manipulating the solvation model and using the CTSR tool. The CTSR tool was effective in identifying a few transition states, but only after the SMD solvation model was disabled.³⁸ Once identified, we re-enabled the SMD model and reoptimized the transition states so that the resulting activation energies would be directly comparable to other values simulated in this experiment. The findings, summarized in Figure 2, show no clear chain length dependence, with activation energies substantially higher for headgroup abstraction—consistent with what we observed for PFCA and FTCA. These results suggest that in the gas phase, hydrogen abstraction from the headgroup is possible, but the side chain is preferred. This has implications for atmospheric degradation mechanisms and could be an early step in forming some of the newly detected PFAS. Additionally, the challenges in simulating this family, closely tied to the solvation model, may indicate a strong dependence of this reaction on the polarization of the headgroup, which is disrupted by the SMD model. We recommend that future studies examine sulfonic acid abstraction in the presence of explicit water molecules, as previously mentioned.

H Atom Abstraction for FTOH and PFAL. FTOH and PFAL were also included in this study for consistency and a possible benchmarking of our computational approach. Prior investigations have comprehensively examined their atmospheric fate and determined the rate constant for hydrogen abstraction by hydroxyl radicals. It has been established in

these previous studies that FTOH molecules eventually undergo transformation into corresponding aldehyde which are eventually converted to PFCA compounds in the atmosphere.^{53,57,58} Consequently, FTOH and PFAL were not simulated broadly in this study, as they can be regarded as precursors to atmospheric PFCA and have already been extensively scrutinized in the existing body of research. Calculated energetics for FTOH and PFAL are included in Tables S3 and S4, respectively.

For FTOH, the activation energy for H-abstraction from the alcohol headgroup (~7.9 kcal/mol) was significantly higher when compared to the abstraction from the side chain (~2.8 kcal/mol). If we use Wallington's measured rate expression for the H-abstraction from α carbon with hydroxyl radical and back calculate the experimental energy barrier we get 5.4 kcal/mol.⁵⁸ This is relatively similar to the 2.8 kcal/mol simulated in this experiment and is reasonable given the assumptions made in this calculation, namely estimating Arrhenius pre-exponential factor and temperature and assuming the measured rate only due to H atom abstraction from α carbon.

Data for simulated PFAL show a similarly low activation energy. Activation energy for the reaction between CF_3CHO and OH radical was 4.9 kcal/mol, which is in excellent agreement with an activation barrier of 4.2 kcal/mol, which was back calculated from a literature rate constant as well.⁵⁹ Another trend that emerges from PFAL data (Table S4) shows the negative impact of fluorination where activation energy increases with the amount of fluorine on the molecule, suggesting they were withdrawing electron density from the aldehyde and making it less reactive toward oxidation. Nonetheless, the agreement of calculated data with previously reported experimental measurements demonstrates the validity of the computational approach utilized here.

H Atom Abstraction for FASA. Sulfonamides shown in Figure S5 were modeled to determine how H-abstraction activation energies were affected by different perfluoroalkyl chains, alkyl headgroups, and abstraction sites. As shown in Figure 4, activation barriers for H atom abstractions from the amine center or *N*-alkyl groups are unaffected by the perfluoroalkyl chain length. H-abstraction from different sites in *N*-ethyl functionality shows that the methylene unit is the most favored site followed by the CH_3 group, making abstraction from the nitrogen center the least favorable. In the case of *N*-methyl functionality, H atom abstraction from the carbon center was more favorable than the nitrogen center.

■ ENVIRONMENTAL IMPLICATIONS

The results from this study showed that the oxidative degradation of various PFAS families in the atmosphere is feasible, the perfluoroalkyl chain length of a molecule does not impact the reaction, and the side chain H-abstraction will be preferred when available.

First, the activation energies of the hydrogen abstraction for every subclass studied are of a similar magnitude (or lower) to those of aqueous phase oxidation, suggesting the reactions are feasible in the atmosphere. As shown in Table S5 summarizing activation energies from this study, the values generally fall below 14.5 kcal/mol. This aligns with experimental values ranging from 13.4 to 25.6 kcal/mol for PFCA oxidation in solution by sulfate radical.^{47–51} For many PFAS families, the activation barriers are substantially below the aforementioned number, particularly for the abstraction of hydrogen from side chains. It should be noted that in the aqueous phase specific

conditions need to be met for oxidative degradation to take place, and one could argue the same difficulty will be present in the atmosphere. However, the key difference is that in the aqueous phase, these difficulties are a result of dealing with the deprotonated form of these chemicals, such as having to manipulate the pH. This contrasts with the atmospheric degradation, which would occur with the protonated forms of the molecules and, therefore, will not have difficulties analogous to the aqueous phase oxidation.

Second, the chain length was found to have no discernible impact on the activation energy in the atmosphere. With degradation mechanisms involving interaction to a surface, such as in electrochemical oxidation, chain length plays a big role, because chain length affects the magnitude of hydrophobic interactions and the solubility of the compounds. This decrease in adsorption probability leads to substantially decreased degradation efficiency for the short-chain and ultrashort-chain PFAS in such systems. However, in the gas phase, no coordination to the support is required. This in conjunction with the lack of chain length dependence in the actual activation energies suggests that in the atmosphere, all of the various chain lengths would degrade at similar rates. Consequently, higher concentrations of short and ultrashort PFAS may be expected in the atmosphere. This could explain recent observations made of exceedingly high short and ultrashort PFAS found in rainwater in certain sites.¹⁹

Third, substances featuring trifluoromethyl substitution at the α carbon position exhibited comparable degradation rates to their nonsubstituted counterparts, albeit with a slight enhancement in degradation rate. The researchers believe the observed trend is too small to overcome the error introduced by the thermal corrections, and it cannot be concluded from these data if it makes a significant difference. This could mean molecules like GenX that are marketed to be easier to degrade because of this substitution are, in fact, just as recalcitrant as the versions of the molecule without a trifluoromethyl substitution in the gas phase.

Finally, side chain abstraction is the preferred pathway that introduces the possibility of generating a diverse array of compounds. While we did not simulate any potential reactions starting from this side chain radical, it is likely that reactions other than the Kolbe decarboxylation will follow. As a result, a multitude of unknown reactions could result from this initial abstraction step and may be responsible for some of the novel compounds being observed. These results are in excellent agreement with studies of FTOH, suggesting the side chain is preferred for even more PFAS families. This side chain abstraction could give rise to a multitude of products that deviate from predictions made by existing methods. The reaction pathways following this side chain abstraction must be studied in more detail to elucidate the new breed of PFAS being created in the atmosphere. These conclusions collectively inform future studies on the fate and transport of PFAS in the atmosphere, offering valuable insights into potential speciation under atmospheric conditions.

■ ASSOCIATED CONTENT

SI Supporting Information

The Supporting Information is available free of charge at <https://pubs.acs.org/doi/10.1021/acsestair.4c00070>.

Additional information about the computational methods used; hindered rotor errors; bottom-of-the-well

energies; conformational analysis; extra PFAS families; α carbon substitution; summary of calculated energies; as well as optimized geometries and energies (PDF)

AUTHOR INFORMATION

Corresponding Author

Shubham Vyas — Department of Chemistry, Colorado School of Mines, Golden, Colorado 80401, United States;
ORCID.org/0000-0002-5849-8919; Email: svyas@mines.edu

Authors

Michael R. Dooley — Department of Chemistry, Colorado School of Mines, Golden, Colorado 80401, United States;
ORCID.org/0009-0007-0244-0324

Steven P. Nixon — Department of Chemistry, Colorado School of Mines, Golden, Colorado 80401, United States

Benjamin E. Payton — Department of Chemistry, Colorado School of Mines, Golden, Colorado 80401, United States

Mikayla A. Hudak — Department of Chemistry, Colorado School of Mines, Golden, Colorado 80401, United States

Fiona Odei — Department of Chemistry, Colorado School of Mines, Golden, Colorado 80401, United States

Complete contact information is available at:

<https://pubs.acs.org/10.1021/acsestair.4c00070>

Author Contributions

[‡]B.E.P. and M.A.H. contributed equally. M.R.D. drafted the initial manuscript. All authors revised the manuscript, contributed scientifically, and approved the final manuscript. S.V. was involved in the conception of the project and the manuscript.

Notes

The authors declare no competing financial interest.

ACKNOWLEDGMENTS

This work was financially supported by the National Science Foundation through AGS-2220845 and CHE-2109210. Financial support from US Army Corp of Engineers through cooperative agreement W912HZ-23-2-0009 is also gratefully acknowledged. Authors also acknowledge the computational resources allocated by the high-performance computing facility at the Colorado School of Mines.

ABBREVIATIONS

PFAS, per- and polyfluoroalkyl substances; PFCA, perfluoroalkyl carboxylic acid; FTCA, fluorotelomer carboxylic acid; FTOH, fluorotelomer alcohol; PFSA, perfluoroalkyl sulfonic acid; FTSA, fluorotelomer sulfonic acid; FASA, fluorotelomer sulfonamide; PFEA, perfluoro ether carboxylic acid; DPFEA, perfluoro diether carboxylic acid; PFAL, perfluoro aldehyde; DFT, density functional theory; IRC, intrinsic reaction coordinate

REFERENCES

- (1) Wang, Z.; DeWitt, J. C.; Higgins, C. P.; Cousins, I. T. A Never-Ending Story of Per- and Polyfluoroalkyl Substances (PFASs)? *Environ. Sci. Technol.* **2017**, *51* (5), 2508–2518.
- (2) Gluge, J.; Scheringer, M.; Cousins, I. T.; DeWitt, J. C.; Goldenman, G.; Herzke, D.; Lohmann, R.; Ng, C. A.; Trier, X.; Wang, Z. An Overview of the Uses of Per- and Polyfluoroalkyl Substances (PFAS). *Environ. Sci. Process. Impacts* **2020**, *22* (12), 2345–2373.
- (3) Gar Alalm, M.; Boffito, D. C. Mechanisms and Pathways of PFAS Degradation by Advanced Oxidation and Reduction Processes: A Critical Review. *Chem. Eng. J.* **2022**, *450*, No. 138352.
- (4) Sunderland, E. M.; Hu, X. C.; Dassuncao, C.; Tokranov, A. K.; Wagner, C. C.; Allen, J. G. A Review of the Pathways of Human Exposure to Poly- and Perfluoroalkyl Substances (PFASs) and Present Understanding of Health Effects. *J. Expo. Sci. Environ. Epidemiol.* **2019**, *29* (2), 131–147.
- (5) Radi, A. B.; et al. Per- and Polyfluoroalkyl Substances: Background Information with Focus on Modeling of Fate and Transport of Per- and Polyfluoroalkyl Substances in Air Media. *J. Environ. Eng.* **2022**, *148*, 03122001.
- (6) Morales-McDevitt, M. E.; Becanova, J.; Blum, A.; Bruton, T. A.; Vojta, S.; Woodward, M.; Lohmann, R. The Air That We Breathe: Neutral and Volatile PFAS in Indoor Air. *Environ. Sci. Technol. Lett.* **2021**, *8* (10), 897–902.
- (7) Johansson, J. H.; Salter, M. E.; Navarro, J. C. A.; Leck, C.; Nilsson, E. D.; Cousins, I. T. Global Transport of Perfluoroalkyl Acids via Sea Spray Aerosol. *Environ. Sci. Process. Impacts* **2019**, *21* (4), 635–649.
- (8) Ahrens, L.; Harner, T.; Shoeib, M.; Lane, D. A.; Murphy, J. G. Improved Characterization of Gas–Particle Partitioning for Per- and Polyfluoroalkyl Substances in the Atmosphere Using Annular Diffusion Denuder Samplers. *Environ. Sci. Technol.* **2012**, *46* (13), 7199–7206.
- (9) Lin, H.; Taniyasu, S.; Yamazaki, E.; Wei, S.; Wang, X.; Gai, N.; Kim, J. H.; Eun, H.; Lam, P. K. S.; Yamashita, N. Per- and Polyfluoroalkyl Substances in the Air Particles of Asia: Levels, Seasonality, and Size-Dependent Distribution. *Environ. Sci. Technol.* **2020**, *54* (22), 14182–14191.
- (10) Faust, J. A. PFAS on Atmospheric Aerosol Particles: A Review. *Environ. Sci. Process. Impacts* **2023**, *25*, 133–150.
- (11) Hartz, W. F.; Björnsdotter, M. K.; Yeung, L. W. Y.; Hodson, A.; Thomas, E. R.; Humby, J. D.; Day, C.; Jogsten, I. E.; Kärrman, A.; Kallenborn, R. Levels and Distribution Profiles of Per- and Polyfluoroalkyl Substances (PFAS) in a High Arctic Svalbard Ice Core. *Sci. Total Environ.* **2023**, *871*, No. 161830.
- (12) Casas, G.; Iriarte, J.; D'Agostino, L. A.; Roscales, J. L.; Martínez-Varela, A.; Vila-Costa, M.; Martín, J. W.; Jiménez, B.; Dachs, J. Inputs, Amplification and Sinks of Perfluoroalkyl Substances at Coastal Antarctica. *Environ. Pollut.* **2023**, *338*, No. 122608.
- (13) Casal, P.; Zhang, Y.; Martin, J. W.; Pizarro, M.; Jiménez, B.; Dachs, J. Role of Snow Deposition of Perfluoroalkylated Substances at Coastal Livingston Island (Maritime Antarctica). *Environ. Sci. Technol.* **2017**, *51* (15), 8460–8470.
- (14) Butt, C. M.; Berger, U.; Bossi, R.; Tomy, G. T. Levels and Trends of Poly- and Perfluorinated Compounds in the Arctic Environment. *Sci. Total Environ.* **2010**, *408* (15), 2936–2965.
- (15) Fenton, S. E.; Ducatman, A.; Boobis, A.; DeWitt, J. C.; Lau, C.; Ng, C.; Smith, J. S.; Roberts, S. M. Per- and Polyfluoroalkyl Substance Toxicity and Human Health Review: Current State of Knowledge and Strategies for Informing Future Research. *Environ. Toxicol. Chem.* **2021**, *40* (3), 606–630.
- (16) De Silva, A. O.; Armitage, J. M.; Bruton, T. A.; Dassuncao, C.; Heiger-Bernays, W.; Hu, X. C.; Kärrman, A.; Kelly, B.; Ng, C.; Robuck, A.; Sun, M.; Webster, T. F.; Sunderland, E. M. PFAS Exposure Pathways for Humans and Wildlife: A Synthesis of Current Knowledge and Key Gaps in Understanding. *Environ. Toxicol. Chem.* **2021**, *40* (3), 631–657.
- (17) Ankley, G. T.; Cureton, P.; Hoke, R. A.; Houde, M.; Kumar, A.; Kurias, J.; Lanno, R.; McCarthy, C.; Newsted, J.; Salice, C. J.; Sample, B. E.; Sepúlveda, M. S.; Steevens, J.; Valsecchi, S. Assessing the Ecological Risks of Per- and Polyfluoroalkyl Substances: Current State-of-the-Science and a Proposed Path Forward. *Environ. Toxicol. Chem.* **2021**, *40* (3), 564–605.
- (18) Jansson, F. Occurrence of Per- and Polyfluorinated Alkyl Substances (PFAS), Including Ultra-Short-Chain Compounds. Seasonal Variation in Rainwater from the Swedish West Coast. Bachelor's Thesis, Örebro University, Örebro, Sweden, 2019.

(19) Kim, Y.; Pike, K. A.; Gray, R.; Sprinkle, J. W.; Faust, J. A.; Edmiston, P. L. Non-Targeted Identification and Semi-Quantitation of Emerging per- and Polyfluoroalkyl Substances (PFAS) in US Rainwater. *Environ. Sci. Process. Impacts* **2023**, *25*, 1771–1787.

(20) Liu, M.; Munoz, G.; Vo Duy, S.; Sauvé, S.; Liu, J. Per- and Polyfluoroalkyl Substances in Contaminated Soil and Groundwater at Airports: A Canadian Case Study. *Environ. Sci. Technol.* **2022**, *56* (2), 885–895.

(21) Gligorovski, S.; Strekowski, R.; Barbati, S.; Vione, D. Environmental Implications of Hydroxyl Radicals (\bullet OH). *Chem. Rev.* **2015**, *115* (24), 13051–13092.

(22) Gonda, N.; Choyke, S.; Schaefer, C.; Higgins, C. P.; Voelker, B. Hydroxyl Radical Transformations of Perfluoroalkyl Acid (PFAA) Precursors in Aqueous Film Forming Foams (AFFFs). *Environ. Sci. Technol.* **2023**, *57* (21), 8053–8064.

(23) Liu, J.; Van Hoomissen, D. J.; Liu, T.; Maizel, A.; Huo, X.; Fernández, S. R.; Ren, C.; Xiao, X.; Fang, Y.; Schaefer, C. E.; Higgins, C. P.; Vyas, S.; Strathmann, T. J. Reductive Defluorination of Branched Per- and Polyfluoroalkyl Substances with Cobalt Complex Catalysts. *Environ. Sci. Technol. Lett.* **2018**, *5* (5), 289–294.

(24) Van Hoomissen, D. J.; Vyas, S. Early Events in the Reductive Dehalogenation of Linear Perfluoroalkyl Substances. *Environ. Sci. Technol. Lett.* **2019**, *6* (6), 365–371.

(25) Etz, B. D.; Mirkovic, M.; Vyas, S.; Shukla, M. K. High-Temperature Decomposition Chemistry of Trimethylsiloxane Surfactants, a Potential Fluorine-Free Replacement for Fire Suppression. *Chemosphere* **2022**, *308*, No. 136351.

(26) Pike, K. A.; Edmiston, P. L.; Morrison, J. J.; Faust, J. A. Correlation Analysis of Perfluoroalkyl Substances in Regional U.S. Precipitation Events. *Water Res.* **2021**, *190*, No. 116685.

(27) Munoz, G.; Liu, J.; Vo Duy, S.; Sauvé, S. Analysis of F-53B, Gen-X, ADONA, and Emerging Fluoroalkylether Substances in Environmental and Biomonitoring Samples: A Review. *Trends Environ. Anal. Chem.* **2019**, *23*, No. e00066.

(28) Frisch, M. J.; Trucks, G. W.; Schlegel, H. B.; Scuseria, G. E.; Robb, M. A.; Cheeseman, J. R.; Scalmani, G.; Barone, V.; Petersson, G. A.; Nakatsuji, H.; Li, X.; Caricato, M.; Marenich, A. V.; Bloino, J.; Janesko, B. G.; Gomperts, R.; Mennucci, B.; Hratchian, H. P.; Ortiz, J. V.; Izmaylov, A. F.; Sonnenberg, J. L.; Williams-Young, D.; Ding, F.; Lipparini, F.; Egidi, F.; Goings, J.; Peng, B.; Petrone, A.; Henderson, T.; Ranasinghe, D.; Zakrewski, V. G.; Gao, J.; Rega, N.; Zheng, G.; Liang, W.; Hada, M.; Ehara, M.; Toyota, K.; Fukuda, R.; Hasegawa, J.; Ishida, M.; Nakajima, T.; Honda, Y.; Kitao, O.; Nakai, H.; Vreven, T.; Throssell, K.; Montgomery, J. A., Jr.; Peralta, J. E.; Ogliaro, F.; Bearpark, M. J.; Heyd, J. J.; Brothers, E. N.; Kudin, K. N.; Staroverov, V. N.; Keith, T. A.; Kobayashi, R.; Normand, J.; Raghavachari, K.; Rendell, A. P.; Burant, J. C.; Iyengar, S. S.; Tomasi, J.; Cossi, M.; Millam, J. M.; Klene, M.; Adamo, C.; Cammi, R.; Ochterski, J. W.; Martin, R. L.; Morokuma, K.; Farkas, O.; Foresman, J. B.; Fox, D. J. *Gaussian16*, Revision C.01; Gaussian Inc.: Wallingford, CT, 2016.

(29) Zhao, Y.; Truhlar, D. G. The M06 Suite of Density Functionals for Main Group Thermochemistry, Thermochemical Kinetics, Noncovalent Interactions, Excited States, and Transition Elements: Two New Functionals and Systematic Testing of Four M06-Class Functionals and 12 Other Functionals. *Theor. Chem. Acc.* **2008**, *120* (1), 215–241.

(30) Marenich, A. V.; Cramer, C. J.; Truhlar, D. G. Universal Solvation Model Based on Solute Electron Density and on a Continuum Model of the Solvent Defined by the Bulk Dielectric Constant and Atomic Surface Tensions. *J. Phys. Chem. B* **2009**, *113* (18), 6378–6396.

(31) Allodi, M. A.; Dunn, M. E.; Livada, J.; Kirschner, K. N.; Shields, G. C. Do Hydroxyl Radical–Water Clusters, OH(H₂O)_n, n = 1–5, Exist in the Atmosphere? *J. Phys. Chem. A* **2006**, *110* (49), 13283–13289.

(32) Petit, A. S.; Harvey, J. N. Atmospheric Hydrocarbon Activation by the Hydroxyl Radical: A Simple yet Accurate Computational Protocol for Calculating Rate Coefficients. *Phys. Chem. Chem. Phys.* **2012**, *14* (1), 184–191.

(33) Viegas, L. P. Simplified Protocol for the Calculation of Multiconformer Transition State Theory Rate Constants Applied to Tropospheric OH-Initiated Oxidation Reactions. *J. Phys. Chem. A* **2021**, *125* (21), 4499–4512.

(34) Viegas, L. P. Exploring the Reactivity of Hydrofluoropolyethers toward OH through a Cost-Effective Protocol for Calculating Multiconformer Transition State Theory Rate Constants. *J. Phys. Chem. A* **2018**, *122* (50), 9721–9732.

(35) Viegas, L. P.; Jensen, F. A Computer-Based Solution to the Oxidation Kinetics of Fluorinated and Oxygenated Volatile Organic Compounds. *Environ. Sci. Atmospheres* **2023**, *3* (5), 855–871.

(36) Arp, H. P. H.; Niederer, C.; Goss, K.-U. Predicting the Partitioning Behavior of Various Highly Fluorinated Compounds. *Environ. Sci. Technol.* **2006**, *40* (23), 7298–7304.

(37) Wang, Z.; MacLeod, M.; Cousins, I. T.; Scheringer, M.; Hungerbühler, K. Using COSMOtherm to Predict Physicochemical Properties of Poly- and Perfluorinated Alkyl Substances (PFASs). *Environ. Chem.* **2011**, *8* (4), 389.

(38) Viegas, L. P.; Galvão, B. R. L. With a Little Help from Our (AI) Friend: A General Transition State Sampling Method for Tropospheric Hydrogen Abstraction Reactions. *Atmos. Environ.* **2024**, *328*, No. 120515.

(39) Mirkovic, M.; Van Hoomissen, D. J.; Vyas, S. Conformational Distributions of Helical Perfluoroalkyl Substances and Impacts on Stability. *J. Comput. Chem.* **2022**, *43* (24), 1656–1661.

(40) Cormanich, R. A.; O'Hagan, D.; Bühl, M. Hyperconjugation Is the Source of Helicity in Perfluorinated N-Alkanes. *Angew. Chem.* **2017**, *129* (27), 7975–7978.

(41) Dzib, E.; Merino, G. The Hindered Rotor Theory: A Review. *WIREs Comput. Mol. Sci.* **2022**, *12* (3), No. e1583.

(42) Smith, S. J.; Lauria, M.; Ahrens, L.; McCleaf, P.; Hollman, P.; Bjälkefors Seroka, S.; Hamers, T.; Arp, H. P. H.; Wiberg, K. Electrochemical Oxidation for Treatment of PFAS in Contaminated Water and Fractionated Foam—A Pilot-Scale Study. *ACS EST Water* **2023**, *3* (4), 1201–1211.

(43) Li, F.; Wei, Z.; He, K.; Blaney, L.; Cheng, X.; Xu, T.; Liu, W.; Zhao, D. A Concentrate-and-Destroy Technique for Degradation of Perfluoroctanoic Acid in Water Using a New Adsorptive Photocatalyst. *Water Res.* **2020**, *185*, No. 116219.

(44) Huang, L.; Dong, W.; Hou, H. Investigation of the Reactivity of Hydrated Electron toward Perfluorinated Carboxylates by Laser Flash Photolysis. *Chem. Phys. Lett.* **2007**, *436* (1), 124–128.

(45) Joudan, S.; De Silva, A. O.; Young, C. J. Insufficient Evidence for the Existence of Natural Trifluoroacetic Acid. *Environ. Sci. Process. Impacts* **2021**, *23* (11), 1641–1649.

(46) Pickard, H. M.; Criscitello, A. S.; Persaud, D.; Spencer, C.; Muir, D. C. G.; Lehnher, I.; Sharp, M. J.; De Silva, A. O.; Young, C. J. Ice Core Record of Persistent Short-Chain Fluorinated Alkyl Acids: Evidence of the Impact From Global Environmental Regulations. *Geophys. Res. Lett.* **2020**, *47* (10), No. e2020GL087535.

(47) Yin, P.; Hu, Z.; Song, X.; Liu, J.; Lin, N. Activated Persulfate Oxidation of Perfluoroctanoic Acid (PFOA) in Groundwater under Acidic Conditions. *Int. J. Environ. Res. Public. Health* **2016**, *13* (6), 602.

(48) Liu, C. S.; Higgins, C. P.; Wang, F.; Shih, K. Effect of Temperature on Oxidative Transformation of Perfluoroctanoic Acid (PFOA) by Persulfate Activation in Water. *Sep. Purif. Technol.* **2012**, *91*, 46–51.

(49) Lee, Y.-C.; Lo, S.-L.; Kuo, J.; Lin, Y.-L. Persulfate Oxidation of Perfluoroctanoic Acid under the Temperatures of 20–40°C. *Chem. Eng. J.* **2012**, *198–199*, 27–32.

(50) Zhang, Y.; Moores, A.; Liu, J.; Ghoshal, S. New Insights into the Degradation Mechanism of Perfluoroctanoic Acid by Persulfate from Density Functional Theory and Experimental Data. *Environ. Sci. Technol.* **2019**, *53* (15), 8672–8681.

(51) Park, S.; Lee, L. S.; Medina, V. F.; Zull, A.; Waisner, S. Heat-Activated Persulfate Oxidation of PFOA, 6:2 Fluorotelomer Sulfonate, and PFOS under Conditions Suitable for in-Situ Groundwater Remediation. *Chemosphere* **2016**, *145*, 376–383.

(52) Javed, H.; Lyu, C.; Sun, R.; Zhang, D.; Alvarez, P. J. J. Discerning the Inefficacy of Hydroxyl Radicals during Perfluoroctanoic Acid Degradation. *Chemosphere* **2020**, *247*, No. 125883.

(53) Ellis, D. A.; Martin, J. W.; De Silva, A. O.; Mabury, S. A.; Hurley, M. D.; Sulbaek Andersen, M. P.; Wallington, T. J. Degradation of Fluorotelomer Alcohols: A Likely Atmospheric Source of Perfluorinated Carboxylic Acids. *Environ. Sci. Technol.* **2004**, *38* (12), 3316–3321.

(54) Kirby, A. J. *Stereoelectronic Effects*; Oxford University Press, 1996.

(55) Anglada, J. M.; Olivella, S.; Solé, A. Hydrogen Transfer between Sulfuric Acid and Hydroxyl Radical in the Gas Phase: Competition among Hydrogen Atom Transfer, Proton-Coupled Electron-Transfer, and Double Proton Transfer. *J. Phys. Chem. A* **2006**, *110* (5), 1982–1990.

(56) Griesser, M.; Chauvin, J.-P. R.; Pratt, D. A. The Hydrogen Atom Transfer Reactivity of Sulfinic Acids. *Chem. Sci.* **2018**, *9* (36), 7218–7229.

(57) Sulbaek Andersen, M. P.; Nielsen, O. J.; Hurley, M. D.; Ball, J. C.; Wallington, T. J.; Ellis, D. A.; Martin, J. W.; Mabury, S. A. Atmospheric Chemistry of 4:2 Fluorotelomer Alcohol (n-C₄F₉CH₂CH₂OH): Products and Mechanism of Cl Atom Initiated Oxidation in the Presence of NO_x. *J. Phys. Chem. A* **2005**, *109* (9), 1849–1856.

(58) Wallington, T. J.; Hurley, M. D.; Xia, J.; Wuebbles, D. J.; Sillman, S.; Ito, A.; Penner, J. E.; Ellis, D. A.; Martin, J.; Mabury, S. A.; Nielsen, O. J.; Sulbaek Andersen, M. P. Formation of C₇F₁₅COOH (PFOA) and Other Perfluorocarboxylic Acids during the Atmospheric Oxidation of 8:2 Fluorotelomer Alcohol. *Environ. Sci. Technol.* **2006**, *40* (3), 924–930.

(59) Sellevåg, S. R.; Kelly, T.; Sidebottom, H.; Nielsen, C. J. A Study of the IR and UV-Vis Absorption Cross-Sections, Photolysis and OH-Initiated Oxidation of CF₃CHO and CF₃CH₂CHO. *Phys. Chem. Chem. Phys.* **2004**, *6* (6), 1243–1252.